Rapid Communications

Analytic representation of F_K/F_π in two loop chiral perturbation theory

B. Ananthanarayan,[1] Johan Bijnens,[2] Samuel Friot,[3,4] and Shayan Ghosh[1]

[1]*Centre for High Energy Physics, Indian Institute of Science, Bangalore 560012, Karnataka, India*
[2]*Department of Astronomy and Theoretical Physics, Lund University, Sölvegatan 14A, SE 223-62 Lund, Sweden*
[3]*Institut de Physique Nucléaire d'Orsay, Université Paris-Sud 11, IN2P3-CNRS, F-91405 Orsay Cedex, France*
[4]*Institut de Physique Nucléaire de Lyon, Université Lyon 1, IN2P3-CNRS, F-69622 Villeurbanne Cedex, France*

(Received 1 December 2017; published 2 May 2018)

We present an analytic representation of F_K/F_π as calculated in three-flavor two-loop chiral perturbation theory, which involves expressing three mass scale sunsets in terms of Kampé de Fériet series. We demonstrate how approximations may be made to obtain relatively compact analytic representations. An illustrative set of fits using lattice data is also presented, which shows good agreement with existing fits.

DOI: 10.1103/PhysRevD.97.091502

I. INTRODUCTION

The spectrum of QCD contains as lightest particles the pseudoscalar octet, and their properties provide a test of its nonperturbative features, including chiral symmetry breaking. Of particular importance is the ratio F_K/F_π, which has been investigated on the lattice even at quark masses that include the physical values [1]. In chiral perturbation theory (ChPT) [2] at two-loops, expressions for F_π and F_K involve certain integrals (sunsets) that are evaluated numerically [3]. In this work, we provide an analytic expression for F_K/F_π, which uses double series derived using Mellin-Barnes (MB) representations of the sunsets, providing a template for easy fitting to lattice simulations.

II. METHODOLOGY

The ratio F_K/F_π in two-loop $SU(3)$ ChPT is given by:

$$\frac{F_K}{F_\pi} = 1 + \left(\frac{F_K}{F_0}\bigg|_{p^4} - \frac{F_\pi}{F_0}\bigg|_{p^4}\right)_{\rm NLO} + \left(\frac{F_K}{F_0}\bigg|_{p^6} - \frac{F_\pi}{F_0}\bigg|_{p^6} - \frac{F_K}{F_0}\bigg|_{p^4}\frac{F_\pi}{F_0}\bigg|_{p^4} + \frac{F_\pi}{F_0}\bigg|_{p^4}^2\right)_{\rm NNLO}. \quad (1)$$

The decay constants F_P $(P = \pi, K)$ may be decomposed as:

$$\frac{F_P}{F_0} = 1 + F_P^{(4)} + (F_P)^{(6)}_{CT} + (F_P)^{(6)}_{\rm loop} + \mathcal{O}(p^8), \quad (2)$$

The $\mathcal{O}(p^6)$ contribution can be subdivided as:

$$F_\pi^4(F_P)^{(6)}_{\rm loop} = d^P_{\rm sunset} + d^P_{\log\times\log} + d^P_{\log} + d^P_{\log\times L_i} + d^P_{L_i} + d^P_{L_i\times L_j}. \quad (3)$$

$d^P_{\rm sunset}$ comprises of the pure sunset integral terms, which are not available fully analytically, and whose determination is the goal of this work. The sunset integral is defined as:

$$H^d_{\{\alpha,\beta,\gamma\}}(m_1^2, m_2^2, m_3^2; p^2) = \frac{(1/i)^2}{(2\pi)^{2d}}\int\frac{d^dq\,d^dr}{[q^2-m_1^2]^\alpha[r^2-m_2^2]^\beta[(q+r-p)^2-m_3^2]^\gamma}. \quad (4)$$

Aside from this basic scalar integral, tensor integrals in which the momenta q_μ and $q_\mu q_\nu$ appear in the numerator, and derivatives of both the scalar and tensor integrals w.r.t. p^2 contribute to $d^P_{\rm sunset}$ [3]. The tensor and derivative integrals, as well as all the derivatives, may be reduced into a linear combination of scalar integrals using the methods given in [4].

The full list of sunset integrals contributing to $d^P_{\rm sunset}$ can thus all be expressed in terms of a set of four master integrals and the one-loop tadpole integral. The problem reduces to solving these analytically in the required mass configurations. For F_K/F_π, seven distinct three mass scale MI need evaluation.

MB theory leads to representations of these MI where each integral consists of at least one double complex plane integral. These double MB integrals are evaluated using the method proposed in [5] and fully systematized in [6] to obtain results in the form of sums of single and double infinite series [7–9].

III. THE ANALYTIC REPRESENTATION

Using Eq. (3), we obtain the following representation of F_K/F_π:

$$\begin{aligned}\frac{F_K}{F_\pi} &= 1 + 4(4\pi)^2 L_5^r(\xi_K - \xi_\pi) + \frac{5}{8}\xi_\pi\lambda_\pi - \frac{1}{4}\xi_K\lambda_K \\ &+ \left(\frac{1}{8}\xi_\pi - \frac{1}{2}\xi_K\right)\lambda_\eta + \xi_K^2 F_F\left[\frac{m_\pi^2}{m_K^2}\right] + \hat{K}_1^r\lambda_\pi^2 \\ &+ \hat{K}_2^r\lambda_\pi\lambda_K + \hat{K}_3^r\lambda_\pi\lambda_\eta + \hat{K}_4^r\lambda_K^2 + \hat{K}_5^r\lambda_K\lambda_\eta \\ &+ \hat{K}_6^r\lambda_\eta^2\xi_K^2 + \hat{C}_1\lambda_\pi + \hat{C}_2\lambda_K + \hat{C}_3\lambda_\eta + \hat{C}_4, \end{aligned} \tag{5}$$

where $\xi_\pi = m_\pi^2/(16\pi^2 F_\pi^2)$, $\xi_K = m_K^2/(16\pi^2 F_\pi^2)$, $\lambda_i = \log(m_i^2/\mu^2)$, and:

$$\begin{aligned} &\hat{K}_1^r = \frac{11}{24}\xi_\pi\xi_K - \frac{131}{192}\xi_\pi^2, \qquad \hat{K}_2^r = -\frac{41}{96}\xi_\pi\xi_K - \frac{3}{32}\xi_\pi^2, \\ &\hat{K}_3^r = \frac{13}{24}\xi_\pi\xi_K + \frac{59}{96}\xi_\pi^2, \qquad \hat{K}_4^r = \frac{17}{36}\xi_K^2 + \frac{7}{144}\xi_\pi\xi_K, \\ &\hat{K}_5^r = -\frac{163}{144}\xi_K^2 - \frac{67}{288}\xi_\pi\xi_K + \frac{3}{32}\xi_\pi^2, \\ &\hat{K}_6^r = \frac{241}{288}\xi_K^2 - \frac{13}{72}\xi_\pi\xi_K - \frac{61}{192}\xi_\pi^2. \end{aligned} \tag{6}$$

$$\begin{aligned} \hat{C}_1^r &= -\left(\frac{7}{9} + \frac{11}{2}(4\pi)^2 L_5^r\right)\xi_\pi\xi_K - \left(\frac{113}{72} + (4\pi)^2\left(4L_1^r + 10L_2^r + \frac{13}{2}L_3^r - \frac{21}{2}L_5^r\right)\right)\xi_\pi^2, \\ \hat{C}_2^r &= \left(\frac{209}{144} + 3(4\pi)^2 L_5^r\right)\xi_\pi\xi_K + \left(\frac{53}{96} + (4\pi)^2(4L_1^r + 10L_2^r + 5L_3^r - 5L_5^r)\right)\xi_K^2, \\ \hat{C}_3^r &= \left(\frac{13}{18} + (4\pi)^2\left(\frac{8}{3}L_3^r - \frac{2}{3}L_5^r - 16L_7^r - 8L_8^r\right)\right)\xi_K^2 - \left(\frac{4}{9} + (4\pi)^2\left(\frac{4}{3}L_3^r + \frac{25}{6}L_5^r - 32L_7^r - 16L_8^r\right)\right)\xi_\pi\xi_K \\ &+ \left(\frac{19}{288} + (4\pi)^2\left(\frac{1}{6}L_3^r + \frac{11}{6}L_5^r - 16L_7^r - 8L_8^r\right)\right)\xi_\pi^2, \\ \hat{C}_4^r &= (4\pi)^2(\xi_K - \xi_\pi)\Big\{8(4\pi)^2(2(C_{14}^r + C_{15}^r)\xi_K + (C_{15}^r + 2C_{17}^r)\xi_\pi) \\ &+ \left(8(4\pi)^2 L_5^r(8L_4^r + 3L_5^r - 16L_6^r - 8L_8^r) - 2L_1^r - L_2^r - \frac{1}{18}L_3^r + \frac{4}{3}L_5^r - 16L_7^r - 8L_8^r\right)\xi_K \\ &+ \left(8(4\pi)^2 L_5^r(4L_4^r + 5L_5^r - 8L_6^r - 8L_8^r) - 2L_1^r - L_2^r - \frac{5}{18}L_3^r - \frac{4}{3}L_5^r + 16L_7^r + 8L_8^r\right)\xi_\pi\Big\}. \end{aligned} \tag{7}$$

F_F consists of terms arising from pure sunset contributions. The split between the $\hat{K}_i$ terms and F_F is not unique: one convenient decomposition, that takes into account the freedom to distribute the chiral logs while keeping the final result unchanged, is

$$\begin{aligned} F_F &= \frac{m_\pi^6}{m_K^6}\left(\frac{49}{48} + \frac{\pi^2}{32}\right) + \frac{m_\pi^4}{m_K^4}\left(\frac{25\,871}{6912} + \frac{919\pi^2}{2592}\right) - \frac{m_\pi^2}{m_K^2}\left(\frac{9875}{864} + \frac{757\pi^2}{1296}\right) + \left(\frac{39\,233}{6912} + \frac{437\pi^2}{1296}\right) \\ &+ \frac{m_K^2}{m_\pi^2}\left(\frac{3}{2} - \frac{\pi^2}{12}\right) - \frac{3}{32}\log^2\left[\frac{m_\pi^2}{m_K^2}\right] - \frac{9}{16}\log\left[\frac{m_\pi^2}{m_K^2}\right] - \frac{1}{8}\frac{m_K^2}{m_\pi^2}\log^2\left[\frac{4}{3} - \frac{m_\pi^2}{3m_K^2}\right] + \frac{5}{64}\frac{m_\pi^6}{m_K^6}\log^2\left[\frac{4m_K^2}{3m_\pi^2} - \frac{1}{3}\right] \\ &+ \frac{(16\pi^2)^2}{m_K^4}(d_{K\pi\pi}^K + d_{K\eta\eta}^K + d_{K\pi\eta}^K - d_{\pi KK}^\pi - d_{\pi\eta\eta}^\pi - d_{KK\eta}^\pi) \end{aligned} \tag{8}$$

where:

$$d_{K\pi\pi}^K = -\left(\frac{27}{64}\frac{m_\pi^4}{m_K^2} + \frac{1}{64}m_K^2 + \frac{9}{16}m_\pi^2\right)\bar{H}_{K\pi\pi}^K + \left(\frac{1}{16}m_K^4 + \frac{1}{8}m_K^2 m_\pi^2 + \frac{9}{16}m_\pi^4\right)\bar{H}_{2K\pi\pi}^K, \tag{9}$$

$$d_{K\eta\eta}^K = -\left(\frac{15}{64}\frac{m_\pi^4}{m_K^2} + \frac{1189}{576}m_K^2 - \frac{65}{48}m_\pi^2\right)\bar{H}_{K\eta\eta}^K + \left(\frac{143}{48}m_K^4 - \frac{139}{72}m_K^2 m_\pi^2 + \frac{5}{16}m_\pi^4\right)\bar{H}_{2K\eta\eta}^K, \tag{10}$$

$$\begin{aligned} d_{K\pi\eta}^K &= \left(-\frac{7}{32}\frac{m_\pi^4}{m_K^2} + \frac{5}{96}m_K^2 + \frac{7}{6}m_\pi^2\right)\bar{H}_{K\pi\eta}^K + \left(\frac{3}{8}\frac{m_\pi^6}{m_K^2} + \frac{1}{4}m_K^2 m_\pi^2 - \frac{15}{8}m_\pi^4\right)\bar{H}_{K2\pi\eta}^K \\ &- \left(\frac{11}{18}m_K^4 - \frac{1}{12}\frac{m_\pi^6}{m_K^2} + \frac{41}{72}m_K^2 m_\pi^2 + \frac{11}{72}m_\pi^4\right)\bar{H}_{K\pi2\eta}^K - \left(\frac{1}{2}m_K^4\right)\bar{H}_{2K\pi\eta}^K, \end{aligned} \tag{11}$$

$$d^{\pi}_{\pi KK} = -\left(\frac{9}{16}\frac{m_K^4}{m_\pi^2} + \frac{3}{4}m_K^2 + \frac{1}{48}m_\pi^2\right)\bar{H}^{\pi}_{\pi KK} + \left(\frac{3}{4}m_K^4 + \frac{1}{6}m_K^2 m_\pi^2 + \frac{1}{12}m_\pi^4\right)\bar{H}^{\pi}_{2\pi KK}, \quad (12)$$

$$d^{\pi}_{\pi\eta\eta} = \left(-\frac{1}{36}m_\pi^2\right)\bar{H}^{\pi}_{\pi\eta\eta} + \left(\frac{1}{36}m_\pi^4\right)\bar{H}^{\pi}_{2\pi\eta\eta}, \quad (13)$$

and

$$d^{\pi}_{KK\eta} = \left(\frac{15}{16}\frac{m_K^4}{m_\pi^2} - \frac{13}{36}m_K^2 + \frac{13}{144}m_\pi^2\right)\bar{H}^{\pi}_{KK\eta} + \left(\frac{91}{108}m_K^4 - \frac{m_K^6}{m_\pi^2} - \frac{5}{27}m_K^2 m_\pi^2 + \frac{m_\pi^4}{108}\right)\bar{H}^{\pi}_{KK2\eta} + \left(\frac{1}{2}m_K^4 - 2\frac{m_K^6}{m_\pi^2} - \frac{1}{6}m_K^2 m_\pi^2\right)\bar{H}^{\pi}_{2KK\eta}. \quad (14)$$

The MI are denoted by $\bar{H}^{S}_{aPbQcR} \equiv \bar{H}^{d}_{\{a,b,c\}}(m_P^2, m_Q^2, m_R^2; p^2 = m_S^2)$, the "bar" indicating that the chiral subtraction prefactor $(\mu^2 \frac{e^{\gamma_E - 1}}{4\pi})^{4-d}$ has been taken into account, and that the chiral logarithms have been extracted and included in the log terms of Eq. (2). Expressions for the two mass scale MI are given in [10], and those for the three mass scale are given below in terms of generalized hypergeometric (${}_pF_q$) and Kampé de Fériet (KdF) series. The three mass scale MI not explicitly presented here can be derived from the following by differentiation w.r.t the appropriate square propagator mass. The validity of Eqs. (15)–(17) is dictated by the region of convergence of the KdF and ${}_pF_q$ series, which is given by $(m_\pi < m_\eta) \wedge (m_\pi + m_\eta < 2m_K)$ and shown in Fig. 1.

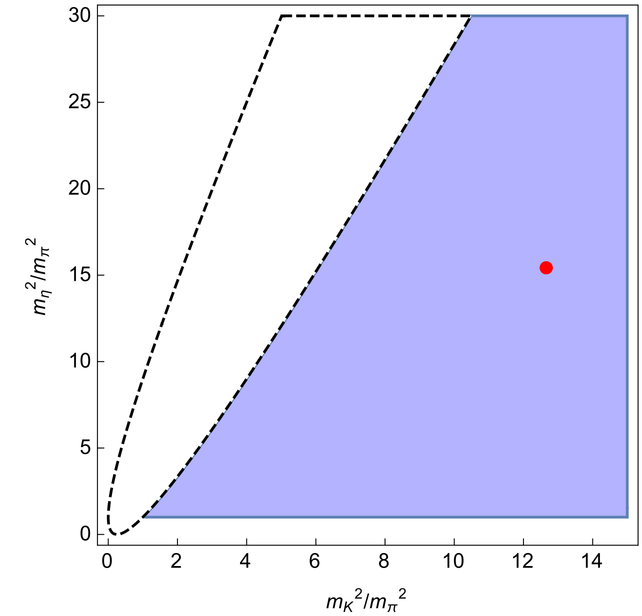

FIG. 1. Region of convergence of Eqs. (15)–(17) (blue region). The red dot marks the physical values of the meson masses.

$$\begin{aligned}
\bar{H}^{K}_{K\pi\eta} = \frac{m_K^2}{512\pi^4}\Bigg\{ & -\frac{7}{4}\left(\frac{m_\eta^4}{m_K^4} + \frac{m_\pi^4}{m_K^4}\right) - \frac{m_\pi^2}{m_K^2}\log\left[\frac{m_\pi^2}{m_K^2}\right]^2 + \left(1 - \frac{\pi^2}{2}\right)\left(\frac{m_\eta^2}{m_K^2} + \frac{m_\pi^2}{m_K^2}\right) + \frac{m_\pi^4}{2m_K^4}\log\left[\frac{m_\pi^2}{m_K^2}\right] - \frac{1}{4} \\
& + \frac{m_\pi^2}{m_K^2}\frac{m_\eta^2}{m_K^2}\left(7 + \frac{2\pi^2}{3} - 2\log\left[\frac{m_\eta^2}{m_K^2}\right] - 2\log\left[\frac{m_\pi^2}{m_K^2}\right] + \log\left[\frac{m_\eta^2}{m_K^2}\right]\log\left[\frac{m_\pi^2}{m_K^2}\right]\right) + \frac{m_\eta^4}{2m_K^4}\log\left[\frac{m_\eta^2}{m_K^2}\right] + \frac{5\pi^2}{6} - \frac{m_\eta^2}{m_K^2}\log\left[\frac{m_\eta^2}{m_K^2}\right]^2 \\
& + \frac{8\pi}{3}\left(\frac{m_\eta^2}{m_K^2}\right)^{3/2} {}_2F_1\left[\left.\begin{matrix}\frac{1}{2}, -\frac{1}{2} \\ \frac{5}{2}\end{matrix}\right| \frac{m_\eta^2}{4m_K^2}\right] + \frac{1}{36}\frac{m_\eta^6}{m_K^6}\,{}_3F_2\left[\left.\begin{matrix}1,1,2 \\ \frac{5}{2},4\end{matrix}\right| \frac{m_\eta^2}{4m_K^2}\right] + \frac{1}{36}\frac{m_\pi^6}{m_K^6}\,{}_3F_2\left[\left.\begin{matrix}1,1,2 \\ \frac{5}{2},4\end{matrix}\right| \frac{m_\pi^2}{4m_K^2}\right] \\
& + \frac{1}{6}\frac{m_\eta^4}{m_K^4}\frac{m_\pi^2}{m_K^2}\left(2\gamma_E - 1 + \log\left[\frac{m_\pi^2 m_\eta^2}{16m_K^4}\right]\right){}_2F_1\left[\left.\begin{matrix}1,1 \\ \frac{5}{2}\end{matrix}\right| \frac{m_\pi^2}{4m_K^2}\right] + \frac{\sqrt{\pi}}{8}\frac{m_\pi^2}{m_K^2}\frac{m_\eta^4}{m_K^4}\left(\log\left[\frac{m_\eta^2}{4m_K^2}\right] + \log\left[\frac{m_\pi^2}{4m_K^2}\right] + \frac{\partial}{\partial\alpha}\right) \\
& \cdot\left(\frac{\Gamma(1+2\alpha)\Gamma(2+2\alpha)\Gamma(3+2\alpha)}{\Gamma(1+\alpha)\Gamma^2(2+\alpha)\Gamma(3+\alpha)\Gamma(\frac{5}{2}+2\alpha)} F^{3:1}_{1:2}\left[\left.\begin{matrix}1+2\alpha, 2+2\alpha, 3+2\alpha : 1,1 \\ \frac{5}{2}+2\alpha : 2+\alpha, 1+\alpha; 3+\alpha, 2+\alpha\end{matrix}\right| \frac{m_\eta^2}{4m_K^2}, \frac{m_\pi^2}{4m_K^2}\right]\right)\Bigg|_{\alpha=0} \\
& - \frac{m_K}{m_\eta}\frac{m_\pi^4}{m_K^4}\left(\log\left[\frac{m_\pi^2}{m_\eta^2}\right] + \frac{\partial}{\partial\alpha}\right)\cdot\left(\frac{\Gamma(\frac{1}{2}+\alpha)\Gamma(\frac{3}{2}+\alpha)}{\Gamma(2+\alpha)\Gamma(3+\alpha)} F^{0:3}_{2:0}\left[\left.\begin{matrix}- : \frac{1}{2}+\alpha, -\frac{1}{2}; \frac{3}{2}+\alpha, \frac{1}{2}; 1, \frac{3}{2} \\ 2+\alpha, 3+\alpha : -\end{matrix}\right| \frac{m_\pi^2}{m_\eta^2}, \frac{m_\pi^2}{4m_K^2}\right]\right)\Bigg|_{\alpha=0} \\
& + \frac{m_\pi^2}{m_K^2}\frac{m_\eta}{m_K}\left(\log\left[\frac{m_\pi^2}{m_\eta^2}\right] + \frac{\partial}{\partial\alpha}\right)\cdot\left(\frac{\pi^2}{\Gamma(\frac{1}{2}-\alpha)\Gamma(\frac{3}{2}-\alpha)\Gamma(1+\alpha)\Gamma(2+\alpha)} F^{3:1}_{1:2}\left[\left.\begin{matrix}-\frac{1}{2}, \frac{1}{2}, \frac{3}{2} : 1,1 \\ 1 : \frac{1}{2}-\alpha, 1+\alpha; \frac{3}{2}-\alpha, 2+\alpha\end{matrix}\right| \frac{m_\eta^2}{4m_K^2}, \frac{m_\pi^2}{4m_K^2}\right]\right)\Bigg|_{\alpha=0} \\
& + \frac{\sqrt{\pi}}{16}\frac{m_\eta^2}{m_K^2}\frac{m_\pi^4}{m_K^4}\frac{\partial}{\partial\alpha}\cdot\left(\frac{\Gamma(1+2\alpha)\Gamma(2+\alpha)\Gamma(3+\alpha)}{\Gamma(\frac{5}{2}+2\alpha)}\,{}_4F_3\left[\left.\begin{matrix}1, 1+2\alpha, 2+\alpha, 3+\alpha \\ 2, 3, \frac{5}{2}+2\alpha\end{matrix}\right| \frac{m_\pi^2}{4m_K^2}\right]\right)\Bigg|_{\alpha=0}\Bigg\},
\end{aligned} \quad (15)$$

$$\bar{H}^K_{2K\pi\eta} = \frac{1}{512\pi^4}\Bigg\{-\frac{m_\eta^2}{m_K^2}\left(1+\frac{\pi^2}{3}+\frac{1}{2}\log^2\left[\frac{m_K^2}{m_\eta^2}\right]+\log\left[\frac{m_K^2}{m_\eta^2}\right]+\mathrm{Li}_2\left[1-\frac{m_\pi^2}{m_\eta^2}\right]\right)$$
$$-\frac{m_\pi^2}{m_K^2}\left(1+\frac{\pi^2}{3}-\log\left[\frac{m_\pi^2}{m_K^2}\right]-\log\left[\frac{m_K^2}{m_\eta^2}\right]\log\left[\frac{m_\pi^2}{m_K^2}\right]-\frac{1}{2}\log^2\left[\frac{m_K^2}{m_\eta^2}\right]-\mathrm{Li}_2\left[1-\frac{m_\pi^2}{m_\eta^2}\right]\right)+\frac{2\pi}{3}\frac{m_\eta^3}{m_K^3}\,{}_2F_1\left[\begin{matrix}\frac{1}{2},\frac{1}{2}\\ \frac{5}{2}\end{matrix}\middle|\frac{m_\eta^2}{4m_K^2}\right]$$
$$-\frac{m_\pi^4}{4m_K^4}\,{}_3F_2\left[\begin{matrix}1,1,1\\ \frac{3}{2},3\end{matrix}\middle|\frac{m_\pi^2}{4m_K^2}\right]-\frac{m_\eta^4}{4m_K^4}\,{}_3F_2\left[\begin{matrix}1,1,1\\ \frac{3}{2},3\end{matrix}\middle|\frac{m_\eta^2}{4m_K^2}\right]-\frac{\sqrt{\pi}}{4}\frac{m_\eta^2}{m_K^2}\frac{m_\pi^2}{m_K^2}\left(\log\left[\frac{m_\pi^2}{4m_K^2}\right]+\log\left[\frac{m_\eta^2}{4m_K^2}\right]+\frac{\partial}{\partial\alpha}\right)$$
$$\cdot\left(\frac{\Gamma^2(1+2\alpha)\Gamma(2+2\alpha)}{\Gamma(\frac{3}{2}+2\alpha)\Gamma^2(1+\alpha)\Gamma^2(2+\alpha)}F^{3:1}_{1:2}\left[\begin{matrix}1+2\alpha,1+2\alpha,2+2\alpha:1,1\\ \frac{3}{2}+2\alpha:1+\alpha,1+\alpha;2+\alpha,2+\alpha\end{matrix}\middle|\frac{m_\eta^2}{4m_K^2},\frac{m_\pi^2}{4m_K^2}\right]\right)\Bigg|_{\alpha=0}$$
$$+\frac{5\pi^2}{6}-1+\frac{\pi^2}{4}\frac{m_\eta}{m_K}\frac{m_\pi^2}{m_K^2}\left(\log\left[\frac{m_\pi^2}{m_\eta^2}\right]+\frac{\partial}{\partial\alpha}\right)$$
$$\cdot\left(\frac{1}{\Gamma(\frac{1}{2}-\alpha)\Gamma(\frac{3}{2}-\alpha)\Gamma(1+\alpha)\Gamma(2+\alpha)}F^{3:1}_{1:2}\left[\begin{matrix}\frac{1}{2},\frac{1}{2},\frac{3}{2}:1,1\\ 1:\frac{1}{2}-\alpha,1+\alpha;\frac{3}{2}-\alpha,2+\alpha\end{matrix}\middle|\frac{m_\eta^2}{4m_K^2},\frac{m_\pi^2}{4m_K^2}\right]\right)\Bigg|_{\alpha=0}$$
$$-\frac{1}{4}\frac{m_\pi}{m_\eta}\frac{m_\pi^3}{m_K^3}\left(\log\left[\frac{m_\pi^2}{m_\eta^2}\right]+\frac{\partial}{\partial\alpha}\right)\cdot\left(\frac{\Gamma(\frac{1}{2}+\alpha)\Gamma(\frac{3}{2}+\alpha)}{\Gamma(2+\alpha)\Gamma(3+\alpha)}F^{0:3}_{2:0}\left[\begin{matrix}-:1,\frac{1}{2};\frac{1}{2}+\alpha,\frac{1}{2};\frac{3}{2}+\alpha,\frac{3}{2}\\ 2+\alpha,3+\alpha:-\end{matrix}\middle|\frac{m_\pi^2}{m_\eta^2},\frac{m_\pi^2}{4m_K^2}\right]\right)\Bigg|_{\alpha=0}\Bigg\}, \quad (16)$$

and

$$\bar{H}^\pi_{KK\eta} = \frac{m_\eta^2}{512\pi^4}\Bigg\{\frac{\pi^2}{6}-5+4\log\left[\frac{m_\eta^2}{m_K^2}\right]-\log^2\left[\frac{m_\eta^2}{m_K^2}\right]+\frac{m_K^2}{m_\eta^2}\left(6+\frac{\pi^2}{3}\right)$$
$$-\frac{1}{18}\frac{m_\pi^2}{m_K^2}\frac{m_\pi^2}{m_\eta^2}\,{}_3F_2\left[\begin{matrix}1,1,2\\ \frac{5}{2},4\end{matrix}\middle|\frac{m_\pi^2}{4m_K^2}\right]+\frac{m_\pi^2}{m_\eta^2}\left(\log\left[\frac{m_K^2}{m_\pi^2}\right]+\frac{5}{4}\right)-\frac{\sqrt{\pi}}{8}\left(\log\left[\frac{m_\eta^2}{4m_K^2}\right]+\frac{\partial}{\partial\alpha}\right)$$
$$\cdot\left(\frac{m_\pi^2}{m_K^2}\frac{\Gamma(3+\alpha)}{\Gamma(\frac{5}{2}+\alpha)}F^{3:1}_{1:2}\left[\begin{matrix}1+\alpha,2+\alpha,3+\alpha:1,1\\ \frac{5}{2}+\alpha:2,1+\alpha;3,2+\alpha\end{matrix}\middle|\frac{m_\pi^2}{4m_K^2},\frac{m_\eta^2}{4m_K^2}\right]+\frac{2m_\eta^2}{m_K^2}\frac{\Gamma(1+\alpha)}{\Gamma(\frac{5}{2}+\alpha)}\,{}_2F_1\left[\begin{matrix}1,1+\alpha\\ \frac{5}{2}+\alpha\end{matrix}\middle|\frac{m_\eta^2}{4m_K^2}\right]\right)\Bigg|_{\alpha=0}\Bigg\}. \quad (17)$$

One may obtain simplified representations for F_F by truncating the series at the desired precision, and taking an expansion around $\rho = \frac{m_\pi^2}{m_K^2} = 0$. For illustrative purposes, we present one such representation in which we truncate the series such that the error between the exact and truncated values is <1% for most of the sets of masses used in the lattice study of [1]. We get:

$$F_F(\rho) = a_1 + (a_2 + a_3\log[\rho] + a_4\log^2[\rho])\rho + (a_5 + a_6\log[\rho] + a_7\log^2[\rho])\rho^2 + (a_8 + a_9\log[\rho] + a_{10}\log^2[\rho])\rho^3 + (a_{11} + a_{12}\log[\rho] + a_{13}\log^2[\rho])\rho^4 + \mathcal{O}(\rho^5) \quad (18)$$

where:

$$a_1 = -\frac{6337}{5184}\left(\mathrm{Li}_2\left[\frac{3}{4}\right]+\log(4)\log\left[\frac{4}{3}\right]\right)+\frac{41\pi^2}{192}-\frac{11\sqrt{2}\pi}{27}+\frac{85\,957\,107\,031}{27\,662\,342\,400}-\frac{119\pi}{216\sqrt{2}}+\frac{62\,591}{6\,12\,360}\log[3]$$
$$+\frac{43\,006\,343}{13\,471\,920}\log\left[\frac{4}{3}\right]+\left(\frac{8\sqrt{2}}{9}-\frac{41\pi}{48}-\frac{5\log[3]}{24\sqrt{2}}\right)\csc^{-1}[\sqrt{3}]+\frac{41}{48}\csc^{-1}[\sqrt{3}]^2+\frac{5}{1152}\log^2\left[\frac{4}{3}\right],$$
$$a_2 = \frac{5821}{2592}\left(\mathrm{Li}_2\left[\frac{3}{4}\right]+\log[4]\log\left[\frac{4}{3}\right]\right)-\frac{25\pi^2}{96}-\frac{7\,269\,419\,973\,251}{1\,120\,324\,867\,200}+\frac{145\pi}{72\sqrt{2}}+\frac{38\,693\pi}{25\,920\sqrt{3}}+\frac{82\gamma}{405}-\frac{121}{576}\log^2\left[\frac{4}{3}\right]$$
$$-\left(\frac{6\,035\,437}{9\,797\,760}+\frac{13\pi}{864\sqrt{3}}\right)\log[3]-\left(\frac{468\,002\,719}{161\,663\,040}+\frac{13\pi}{576\sqrt{3}}\right)\log\left[\frac{4}{3}\right]-\frac{29}{324}\psi\left[\frac{5}{2}\right]$$
$$+\left(\frac{463\log[3]}{384\sqrt{2}}+\frac{\log[\frac{4}{3}]}{2\sqrt{2}}-\frac{11\pi}{48}-\frac{13\gamma}{18\sqrt{2}}-\frac{15\,875}{3456\sqrt{2}}\right)\csc^{-1}[\sqrt{3}]+\frac{11}{48}\csc^{-1}[\sqrt{3}]^2,$$
$$a_3 = \frac{803}{810}+\frac{13\pi}{1728\sqrt{3}}+\frac{7}{48}\log\left[\frac{4}{3}\right]-\frac{1}{2\sqrt{2}}\csc^{-1}[\sqrt{3}], \qquad a_4 = -\frac{11}{24}, \qquad a_7 = \frac{337}{384}, \qquad a_{10} = -\frac{9}{64}, \qquad a_{13} = -\frac{27}{128}$$

$$
\begin{aligned}
a_5 &= \frac{47}{128}\log^2\left[\frac{4}{3}\right] - \frac{845}{648}\left(\mathrm{Li}_2\left[\frac{3}{4}\right] + \log[4]\log\left[\frac{4}{3}\right]\right) - \frac{1301\sqrt{3}\pi}{512} - \frac{66191\gamma}{12960} + \frac{1576413731881}{3585039575040} + \frac{5\pi^2}{18} - \frac{145\pi}{144\sqrt{2}} \\
&\quad + \frac{3572063\pi}{663552\sqrt{3}} + \frac{59}{48}\csc^{-1}[\sqrt{3}]^2 + \left(\frac{744674317}{313528320} + \frac{176189\pi}{55296\sqrt{3}}\right)\log[3] + \frac{35}{144}\psi\left[\frac{5}{2}\right] \\
&\quad + \left(\frac{97621}{55296\sqrt{2}} - \frac{59\pi}{48} + \frac{3167\gamma}{288\sqrt{2}} - \frac{19589\log[3]}{4096\sqrt{2}} - \frac{115}{48\sqrt{2}}\right)\log\left[\frac{4}{3}\right]\csc^{-1}[\sqrt{3}] + \left(\frac{4312709021}{1293304320} + \frac{176189\pi}{36864\sqrt{3}}\right)\log\left[\frac{4}{3}\right], \\
a_6 &= \frac{17003}{8640} - \frac{176189\pi}{110592\sqrt{3}} - \frac{155}{192}\log\left[\frac{4}{3}\right] + \frac{115}{48\sqrt{2}}\csc^{-1}[\sqrt{3}], \\
a_8 &= \frac{265}{864}\left(\mathrm{Li}_2\left[\frac{3}{4}\right] + \log[4]\log\left[\frac{4}{3}\right]\right) + \frac{199393\gamma}{138240} + \frac{25001310633017}{9481096396800} + \frac{4753\pi}{13824\sqrt{2}} + \frac{20910563\pi}{26542080\sqrt{3}} - \frac{29\pi^2}{288} \\
&\quad - \left(\frac{101313035}{143327232} + \frac{804611\pi}{442368\sqrt{3}}\right)\log[3] - \left(\frac{129118553}{117573120} + \frac{804611\pi}{294912\sqrt{3}}\right)\log\left[\frac{4}{3}\right] - \frac{119}{288}\psi\left[\frac{5}{2}\right] - \frac{5}{16}\csc^{-1}[\sqrt{3}]^2 \\
&\quad + \csc^{-1}[\sqrt{3}]\left(\frac{823}{3072\sqrt{2}}\log\left[\frac{4}{3}\right] + \frac{5\pi}{16} - \frac{19319\gamma}{9216\sqrt{2}} - \frac{5341499}{3538944\sqrt{2}} + \frac{104075\log[3]}{196608\sqrt{2}}\right), \\
a_9 &= -\frac{8327}{138240} + \frac{804611\pi}{884736\sqrt{3}} - \frac{1}{96}\log\left[\frac{4}{3}\right] - \frac{823}{3072\sqrt{2}}\csc^{-1}[\sqrt{3}], \\
a_{11} &= -\frac{5}{192}\left(\mathrm{Li}_2\left[\frac{3}{4}\right] + \log[4]\log\left[\frac{4}{3}\right]\right) - \frac{25\pi^2}{192} - \frac{1310311\gamma}{6635520} - \frac{10567863311827}{10113169489920} + \frac{4453\sqrt{3}\pi}{65536} \\
&\quad + \left(\frac{12616533707}{45864714240} + \frac{1674775\pi}{7077888\sqrt{3}}\right)\log[3] + \left(\frac{17720699}{46448640} + \frac{1674775\pi}{4718592\sqrt{3}}\right)\log\left[\frac{4}{3}\right] - \frac{13905571\pi}{84934656\sqrt{3}} \\
&\quad - \frac{2135\pi}{73728\sqrt{2}} + \frac{97}{648}\psi\left[\frac{5}{2}\right] + \frac{1}{\sqrt{2}}\left(\frac{605645}{18874368} - \frac{391\gamma}{49152} - \frac{121093\log[3]}{4194304} - \frac{59}{4096}\log\left[\frac{4}{3}\right]\right)\csc^{-1}[\sqrt{3}], \\
a_{12} &= \frac{5538437}{11612160} - \frac{1674775\pi}{14155776\sqrt{3}} + \frac{1}{64}\log\left[\frac{4}{3}\right] + \frac{59}{4096\sqrt{2}}\csc^{-1}[\sqrt{3}]. \qquad (19)
\end{aligned}
$$

The range of validity of Eqs. (18)–(20) is shown in Fig. 2, in which the exact value of F_F is plotted against $x = \sqrt{\rho}$, as are the approximate F_F retained up to various orders of ρ. The expansion up to $\mathcal{O}(\rho^4)$ approximates the exact value of F_F to 1% for $m_\pi/m_K < 3$ and to 6% for $m_\pi/m_K < 0.5$. One may obtain a representation with greater accuracy by truncating the series with a larger number of terms.

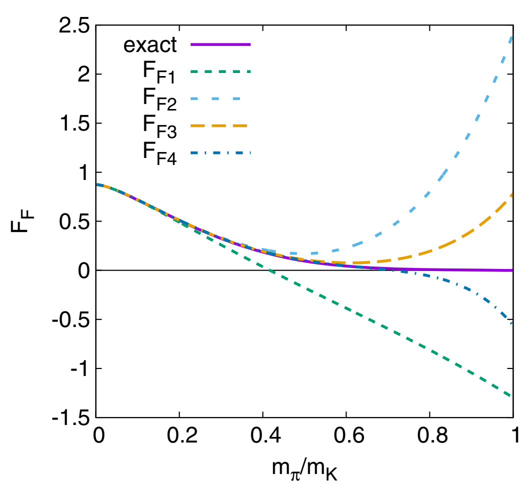

FIG. 2. Comparison of the exact and approximate F_F.

For the reader to be able to verify the implementation of these expressions, we give the numerical values of F_K/F_π coming from both exact and approximate expressions and obtained with physical values $m_\pi = 0.1350$ GeV, $m_K = 0.4955$ GeV, $F_\pi = 0.0922$ GeV, as well as the LEC values of the BE14 fit of [11]. We get, using Eq. (8),

$$F_K/F_\pi = 1.19897, \qquad (20)$$

and using the approximation of Eqs. (18)–(20),

$$F_K/F_\pi = 1.20071. \qquad (21)$$

IV. ILLUSTRATIVE LATTICE FITS

We present an exploratory numerical study based on our analytical representation by fitting Eq. (5) with the data of the lattice study [1] to determine best-fit values of the NLO LEC L_5^r and the NNLO LEC combinations $C_{14}^r + C_{15}^r$ and

TABLE I. Correlation values of the fit in (22).

	L_5	$C_{14}+C_{15}$
$C_{14}+C_{15}$	−0.93	1.00
$C_{15}+2C_{17}$	0.35	−0.66

$C^r_{15}+2C^r_{17}$. We perform the fit (using [12]) on the mass sets for which $m_\pi < 0.40$ GeV. We do the fit on the 'exact' F_F, i.e. truncating the KdF series after 1000^2 terms and the ${}_pF_q$ series after 1000 terms, and cross-check by fitting the exact purely numerical version of Eq. (3) with CHIRON [13]. The fit on the approximate version presented in Eq. (18) gives compatible results.

The uncertainties on the values of the LEC given in this section derive from the errors of the F_K/F_π data of the lattice study, but do not take into account other uncertainties. As detailed in [1], systematic effects due to lattice artificats can arise from correlator fit time choices, lattice spacings, renormalization and finite volume corrections, among other things. When these effects are taken into account, using e.g. [14,15], the values of the LEC presented in this section are likely to change. However, determining the exact nature and magnitude of the change involves a detailed study that is outside the scope of this paper.

We fix the renormalization scale μ at $m_\rho = 0.77$ GeV, and use the values of the BE14 fit [11] for the other L^r_i. In addition we fix F_π in the determination of ξ_π and ξ_K to 92.2 MeV and obtain:

$$L^r_5 = (3.92 \pm 0.55)10^{-4}$$
$$C^r_{14}+C^r_{15} = (2.59 \pm 0.63)10^{-6}$$
$$C^r_{15}+2C^r_{17} = (6.10 \pm 1.41)10^{-6}. \quad (22)$$

The correlation parameters are given in Table I and the quality of the fit is shown in Fig. 3 (Left). The correlation is shown graphically in Fig. 3 (Middle, Right) by plotting a number of random points in a distribution given by the correlation matrix of the fit projected on the two different planes.

With these LEC values and the physical meson masses as inputs, we get for the value of F_K/F_π:

$$F_K/F_\pi = 1.194, \quad (23)$$

which agrees well with the literature value of [11].

The values of Eq. (22) differ from those of the BE14 exact fit ($L_5 = 10.1\times10^{-4}$, $C_{14}+C_{15} = -4.00\times10^{-6}$, $C_{15}+2C_{17} = -5.00\times10^{-6}$) significantly, but are more compatible with those of [16] ($L_5 = 0.76\times10^{-3}$, $C_{14}+C_{15} = 3.15\times10^{-6}$, $C_{15}+2C_{17} = 10.96\times10^{-6}$ in dimensionaless units) and [17] ($L_5 = 0.75\times10^{-3}$, $C_{14}+C_{15} = 1.70\times10^{-6}$, $C_{15}+2C_{17} = 6.04\times10^{-6}$).

A similar fit, but now with F_π also varied in ξ_π, ξ_K requires the use of lattices common to [1,18] to obtain the values of F_π for each lattice. This fit gives:

$$L^r_5 = (0.49 \pm 1.08)10^{-4}$$
$$C^r_{14}+C^r_{15} = (5.59 \pm 1.08)10^{-6}$$
$$C^r_{15}+2C^r_{17} = (39.7 \pm 2.10)10^{-6}. \quad (24)$$

The change in the values above arises primarily due to the variation of F_π. Keeping F_π fixed at 92.2 MeV but with the set of inputs used to calculate Eq. (24) results in changes of ≈20%, 35% and 10% in the Eq. (22) values of the L^r_5, $C^r_{14}+C^r_{15}$ and $C^r_{15}+2C^r_{17}$, respectively. As the difference in the inputs for Eqs. (22) and (24) is primarily the data from the coarsest lattices, it seems that the lattice data has a significant impact on fitting the LECs.

V. CONCLUSIONS

The ratio F_K/F_π is a quantity at the heart of chiral symmetry breaking, a fundamental property of the strong interactions that is measured in *ab initio* calculations on the lattice. An analytic expansion for this quantity in quark or meson masses is the order of the day. Using modern loop calculation techniques, we have achieved this goal. At present, two-loop precision is sufficient to fit the lattice data; this might change when the lattice precision improves in the future. While there exist three-loop results in two-flavor ChPT [19], in three-flavor ChPT two-loops is state of

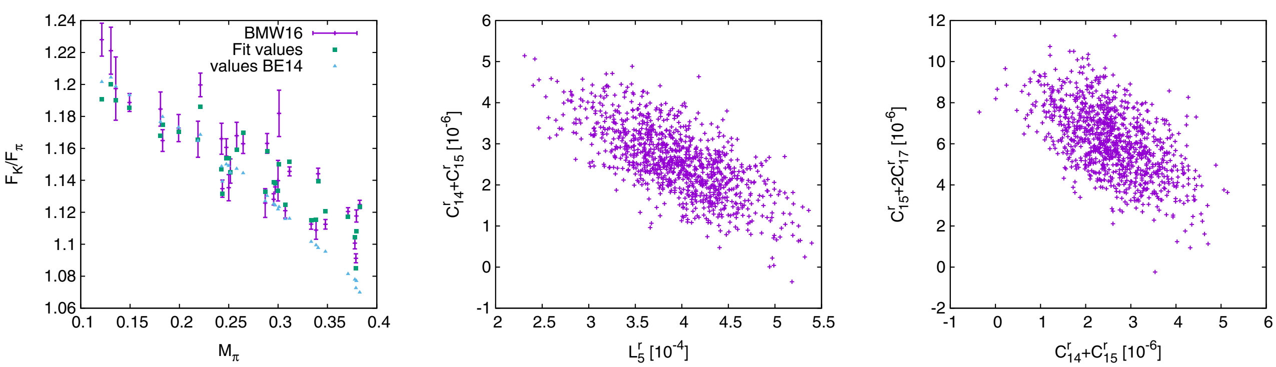

FIG. 3. Left: Quality of the fit. 'Values BE14' plots use the BE14 numbers for L^r_5, C^r_{14}, C^r_{15} and C^r_{17}. Middle: Correlation of L^r_5 and $C^r_{14}+C^r_{15}$. Right: Correlation of $C^r_{14}+C^r_{15}$ and $C^r_{15}+2C^r_{17}$.

the art, adding to the significance of the results presented herein. We hope this work encourages similar cross-disciplinary studies of other quantities of interest.

ACKNOWLEDGMENTS

We thank Pere Masjuan for helpful correspondance regarding the LECs. J. B. is supported in part by the Swedish Research Council Grants Contracts No. 621-2013-4287, No. 2015-04089 and No. 2016-05996 and by the European Research Council under the European Union's Horizon 2020 research and innovation programme (Grant Agreement No. 668679). B. A. is partly supported by the MSIL Chair of the Division of Physical and Mathematical Sciences, Indian Institute of Science.

[1] S. Dürr *et al.*, Leptonic decay-constant ratio f_K/f_π from lattice QCD using $2+1$ clover-improved fermion flavors with 2-HEX smearing, Phys. Rev. D **95**, 054513 (2017).
[2] J. Gasser and H. Leutwyler, Chiral perturbation theory: Expansions in the mass of the strange quark, Nucl. Phys. **B250**, 465 (1985).
[3] G. Amoros, J. Bijnens, and P. Talavera, Two point functions at two loops in three flavor chiral perturbation theory, Nucl. Phys. **B568**, 319 (2000).
[4] O. V. Tarasov, Generalized recurrence relations for two loop propagator integrals with arbitrary masses, Nucl. Phys. **B502**, 455 (1997).
[5] J. P. Aguilar, D. Greynat, and E. De Rafael, Muon anomaly from lepton vacuum polarization and the Mellin-Barnes representation, Phys. Rev. D **77**, 093010 (2008).
[6] S. Friot and D. Greynat, On convergent series representations of Mellin-Barnes integrals, J. Math. Phys. (N.Y.) **53**, 023508 (2012).
[7] B. Ananthanarayan, J. Bijnens, S. Ghosh, and A. Hebbar, An analytic approach to sunset diagrams in chiral perturbation theory: Theory and practice, Eur. Phys. J. A **52**, 374 (2016).
[8] B. Ananthanarayan, J. Bijnens, S. Friot, and S. Ghosh Analytic representations of the heavy pseudoscalar meson masses and decay constants in 2-loop SU(3) ChPT (to be published).
[9] B. Ananthanarayan, S. Friot, and S. Ghosh A mathematical exploration of sunset integrals appearing in eta-related two-loop SU(3) ChPT expressions (to be published).
[10] B. Ananthanarayan, J. Bijnens, and S. Ghosh, An analytic analysis of the pion decay constant in three-flavoured chiral perturbation theory, Eur. Phys. J. C **77**, 497 (2017).
[11] J. Bijnens and G. Ecker, Mesonic low-energy constants, Annu. Rev. Nucl. Part. Sci. **64**, 149 (2014).
[12] F. James and M. Roos, Minuit: A system for function minimization and analysis of the parameter errors and correlations, Comput. Phys. Commun. **10**, 343 (1975).
[13] J. Bijnens, CHIRON: a package for ChPT numerical results at two loops, Eur. Phys. J. C **75**, 27 (2015).
[14] G. Colangelo, S. Durr, and R. Sommer, Finite size effects on M(pi) in QCD from chiral perturbation theory, Nucl. Phys. B, Proc. Suppl. **119**, 254 (2003).
[15] G. Colangelo, S. Durr, and C. Haefeli, Finite volume effects for meson masses and decay constants, Nucl. Phys. **B721**, 136 (2005).
[16] G. Ecker, P. Masjuan, and H. Neufeld, Chiral extrapolation and determination of low-energy constants from lattice data, Phys. Lett. B **692**, 184 (2010).
[17] G. Ecker, P. Masjuan, and H. Neufeld, Approximating chiral $SU(3)$ amplitudes, Eur. Phys. J. C **74**, 2748 (2014).
[18] S. Dürr *et al.* (Budapest-Marseille-Wuppertal Collaboration), Lattice QCD at the physical point meets SU(2) chiral perturbation theory, Phys. Rev. D **90**, 114504 (2014).
[19] J. Bijnens and N. H. Truedsson, The pion mass and decay constant at three loops in two-flavour chiral perturbation theory, J. High Energy Phys. 11 (2017) 181.